33rd Annual International Conference of the IEEE EMBS
Boston, Massachusetts USA, August 30 - September 3, 2011

Numerical Simulation of Motion-induced Dynamic Noise in a Ubiquitous ECG Application

Young Tae Kim, Ki Moo Lim, Seong Bae Hong, Ah Jin Ryu, Byung Hoon Ko, Sang Kon Bae, Kun Soo Shin, and Eun Bo Shim*

***Abstract*— Wearable ubiquitous biomedical applications, such as ECG monitors, can generate dynamic noise as a person moves. However, the source of this noise is not clear. We postulated that the dynamic ECG noise has two causes: the change in displacement of the heart during motion and the change in the electrical impedance of the skin-gel interface due to motion-induced deformation of the skin-gel interface. Using a three-dimensional electrophysiological heart model coupled with a torso model, dynamic noise was simulated, while the displacement of the heart was changed in the vertical and horizontal directions, independently and while the skin-gel interface was deformed during motion. To determine the deformation rate of the skin and sol-gel layers, motion-induced deformation of the two layers was simulated using a three-dimensional finite element method.**

I. Introduction

Motion-induced dynamic noise is a critical issue in electrocardiography (ECG) devices. For wearable ubiquitous biomedical applications, the devices are usually designed to be worn by directly attaching an electrode patch to the skin surface, enabling one to move freely. Therefore, the possibility of motion-induced dynamic noise becomes more critical [1]–[2].

One reason that motion-induced dynamic noise is an intricate problem is that the noise occurs with great uncertainty with various dynamic environmental changes due to motion or an electrode movement artifact at the skin-electrode interface, reducing the reliability of the ECG device. It is very difficult to identify the effect of each noise source in the ECG signal independently because they are usually coupled.

Corresponding author: Eun Bo Shim is with the Department of Mechanical & Biomedical Engineering, Kangwon National University, Chuncheon, Gangwon-do, South Korea. (phone: 82-33-250-6318; e-mail: ebshim@kangwon.ac.kr; fax: 82-33-257-6595)

Young Tae Kim is with the Department of Mechanical & Biomedical Engineering, Kangwon National University, Chuncheon, Ganwon-do, South Korea (bong@yonsei.ac.kr).

Ki Moo Lim is with the Department of Mechanical & Biomedical Engineering, Kangwon National University, Chuncheon, Ganwon-do, South Korea (kmlimphd@gmail.com).

Seong Bae Hong is with the Department of Mechanical & Biomedical Engineering, Kangwon National University, Chuncheon, Ganwon-do, South Korea (seungbae@kangwon.ac.kr).

Byung Hoon Ko is with the Samsung Electronics, Yongin, Gyunggi-do, South Korea (byunghoon.ko@samsung.com).

Sang Kon Bae is with the Samsung Electronics, Yongin, Gyunggi-do, South Korea (sk111.bae@samsung.com).

Kun Soo Shin is with the Samsung Electronics, Yongin, Gyunggi-do, South Korea (bosco.shin@samsung.com).

Several studies have examined dynamic ECG noise [3]–[7], although many of these focused on electronic filtering of the dynamic noise from the ECG signal during motion. In particular, Sameni *et al*. [8] studied a multichannel ECG and noise model under dynamic conditions. They examined the ECG signals of women with multiple pregnancies and the temporal movement and rotation of the cardiac dipoles of the mothers and fetuses. They did not consider more dynamic conditions, such as walking or running.

We postulated that there were two major causes of the motion-induced noise of a ubiquitous ECG device using a bipolar wearable sol-gel patch electrode: the change in the displacement of the heart while walking or running and the change in electrical impedance at the skin-gel interface.

Although it is important to understand the dynamic ECG noise related to heart motion, few studies have examined the effect of heart displacement on such noise. Therefore, we investigated the interference of the ECG waveform due to walking or running motions using a numerical method. The walking and running motions were modeled as vibration of the heart at frequencies of 2~5 Hz. For the numerical investigation, a three-dimensional heart-torso coupled (3DHT) model was developed to map the electrical potential on the 3D surface of a torso model, and motion-induced noise of the ECG signal was simulated.

The change in electrical impedance at the skin-gel (skin and sol-gel layers) interface due to motion-induced deformation of the interface was studied during motion while wearing a sol-gel ECG patch. There are many possible sources of dynamic noise related to the interface between the ECG electrode and the skin surface, such as the change in the half-cell potential of the sol-gel layer. We focused on the change in deformation-induced impedance of the skin-gel interface because motion-induced deformation of the layers can change the mechanical-electronic coupling parameters, such as the electrical resistance and capacitance of the interface.

II. Method

A. 3D electrophysiological heart-torso coupled model and vibrating heart motion

To build a heart model, 3D atrial tissue and ventricular tissue models were linked using a mono-domain method. The following partial differential equation shows the mono-domain heart model for the reaction-diffusion form:

$$\frac{\partial V_m}{\partial t} = \nabla \cdot \left(D\left(\sigma_{mL}, \sigma_{mT}\right) \nabla V_m \right) - I_m \quad (1)$$

where V_m is the membrane voltage, t is time; D is the diffusion tensor of electric wave propagation; σ_{mL} and σ_{mT} are the conductivities parallel and perpendicular to the fiber axis, respectively; and I_m is the membrane current, which is formulated differently according to cell type. All of the parameters and variables of I_m in atrial and ventricular cells are based on Nygren *et al*. [9] and Bueno-Orovio *et al*. [10], respectively.

To create an electrical potential map on the torso surface from the heart model, the BE model of the human torso (Potse *et al*. [11]) was used. The following equation shows the potential $\phi_{ek}(r)$ at point r on the torso surface k:

$$\phi_{ek}(r) = \frac{1}{2\pi\left(\sigma_k^- + \sigma_k^+\right)} \cdot \left[\int J_c(r') \cdot \frac{r - r'^3}{|r - r'|^3} dV' + \sum_l \int_{Sl} \left(\sigma_l^- - \sigma_l^+\right) \phi_e(r'') d\Omega_{rr''} \right] \quad (2)$$

where σ^-_k and σ^+_k indicate the conductivity at the inside and outside surfaces of k, respectively; J_c is the source current density field; r' and r'' are variables; and $d\Omega_{rr''}$ is the solid angle subtended at r by the infinitesimal surface element situated at r''.

The 3DHT model was built with the 3D heart and torso models to simulate motion-induced ECG noise due to motion of the heart, as shown in Fig. 1. Heart motion was generated at 2, 3, and 5 Hz frequencies ($f=\omega/2\pi$) in the vertical and horizontal directions, assuming that the heart moves vertically and horizontally during walking, running, or other motions. The vibration amplitude, A (3), was assumed to be 3 cm in both the vertical and horizontal directions.

$$y = A \cdot sin(\omega \cdot t) \quad (3)$$

During motion of the heart, ECG waveforms were obtained at points a and b, 5 cm apart (Fig. 1), and the normal ECG waveform at rest was subtracted from the ECG values with noise to extract the motion-induced noise waveforms for each case.

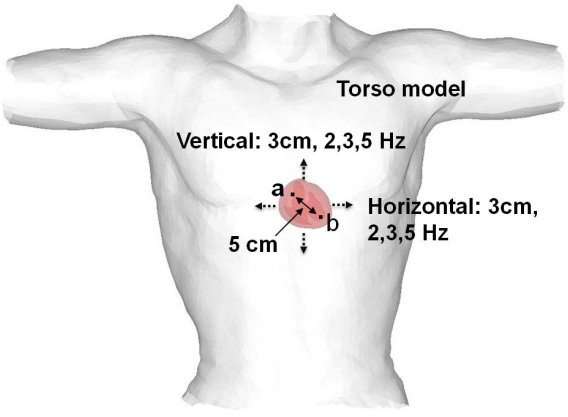

Fig. 1. The 3D heart-torso coupled model and the vibration directions of heart motion while walking or running.

B. Lumped parameter impedance model of the skin-gel interface

As shown in Fig. 2(a), the electrodes (two signal electrodes with a ground at the center) of the bipolar ECG device are connected to the skin surface using a sol-gel layer to ensure conductivity. Flexible, soft polyethylene (PE) foam is used with an adhesive for tight adhesion and conformal contact between the skin surface and ECG device. Based on the layered structure of the contact interface, the electrical impedance of the contact interface was modeled with the electrical lumped parameters R and C, as shown in Fig. 1(b), where R_1, R_2, and R_3 are the resistances of the skin layer, sol-gel layer, and ECG device input, respectively, and C_1 and C_2 are the capacitances of the two layers. The values of R_1, R_2, C_1, and C_2 can be determined using the following equations:

$$R = \rho \frac{L}{A} \quad (4)$$

$$C = \varepsilon_r \varepsilon_0 \frac{A}{L} \quad (5)$$

Consequently, if the specific resistance (ρ), relative static permittivity (ε_r), and electric constant (ε_0) are invariant for the two layers, and the contact area between the skin surface and sol-gel layer are also nearly constant during motion, R and C are designated only by the thickness L (d_1 and d_2) of each layer. Hence, the change in impedance of the skin-gel interface can be determined by measuring the motion-induced deformation of the layers. In the lumped parameter impedance model (Fig. 1(b)), the following two governing equations, (6) and (7) can be derived for the ionic current through the layers.

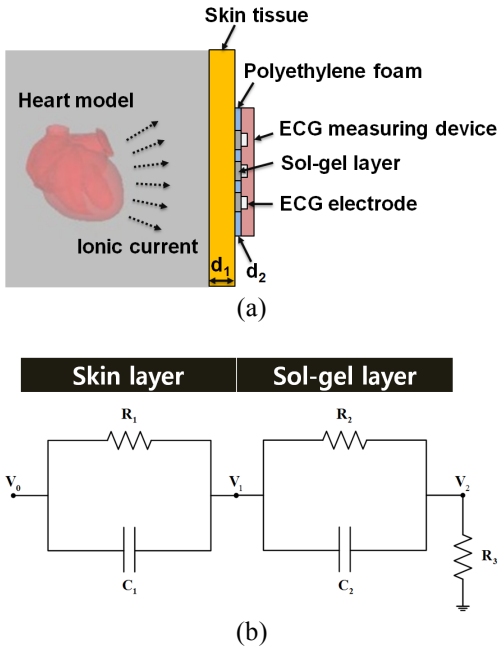

Fig. 2. (a) Cross-sectional schematic of a wearable ECG device attached to the torso model and (b) a lumped parameter impedance model of the skin-gel interface.

$$\frac{V_0 - V_1}{R_1} + C_1 \frac{d}{dt}(V_0 - V_1) - \frac{V_1 - V_2}{R_2} - C_2 \frac{d}{dt}(V_1 - V_2) = 0 \quad (6)$$

$$\frac{V_1 - V_2}{R_2} + C_2 \frac{d}{dt}(V_1 - V_2) - C_1 \frac{dV_2}{dt} = 0 \quad (7)$$

C. *FEM model for motion-induced deformation of the skin-gel interface*

To achieve the correct change in thickness (d_1 and d_2) due to motion-induced deformation of the skin and sol-gel layers and apply the changed values to the lumped parameter impedance model, a skin-gel interface that includes skin tissue, the sol-gel layer, PE foam, and the ECG device was modeled in three dimensions to calculate the deformation of the layers numerically, as shown in Fig. 3.

Based on the wearing conditions of the bipolar ECG device and the motion of the body, a 1-N compressive force was applied perpendicularly to the center of the ECG device and a 10-mm stretch of the skin layer was assumed to take into account skin stretch during motion. The Ogden model of the hyperelasticity of human skin tissue was applied based on Flynn *et al*. [12]. The hyperelastic properties of the sol-gel and PE foams were approximated experimentally for the Ogden model, as shown in the following equation:

$$W = \frac{2\mu}{\alpha^2}(\lambda_1^\alpha + \lambda_2^\alpha + \lambda_3^\alpha) - p(J-1) \quad (8)$$

where μ and α are material parameters; λ_1, λ_2, and λ_3 are the principal stretches; p is a Lagrange multiplier representing hydrostatic pressure; and J is the volume ratio.

From the two compressive and stretch simulations, the dynamic deformation rates of the skin and sol-gel layers were determined at points a and b, the centers of the two sol-gel foams, and the deformation rates were applied to the lumped parameter impedance model to calculate the change in impedance at the skin-gel interface.

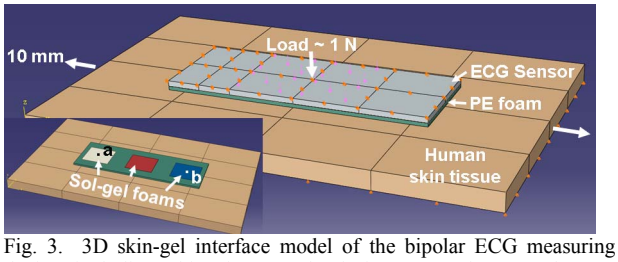

Fig. 3. 3D skin-gel interface model of the bipolar ECG measuring device including skin tissue, sol-gel foam, PE foam, and ECG measuring device.

III. Results

NSR values of the ECG waveforms due to heart vibration were calculated by the lumped parameter impedance model of the skin-gel interface (Fig. 2(b)) for two different directions of motion and three different frequencies as represented in Table1.

Table 1
NSR of the ECG waveforms due to heart vibration

Frequency (Hz)	*2*	*3*	*5*
3-cm vertical motion	0.44	0.22	0.44
3-cm horizontal motion	0.41	0.27	0.55

The ECG waveform between points a and b (Fig. 1) was calculated from the 3DHT model during vibration motion of the heart with a 3-cm amplitude in both the vertical and horizontal directions at frequencies of 2, 3, and 5 Hz. Fig. 4(a) shows the noisy ECG waveform during 3-cm vertical vibration of the heart at 5 Hz and Fig. 4(b) shows the normal ECG waveform at rest. In all cases, the normal ECG value at rest with the heart beating without translational vibration was subtracted from the noisy ECG values to extract the motion-induced dynamic noise because the noisy ECG includes both the signal and noise. To evaluate the noise level, the noise-to-signal ratio (NSR) was calculated by dividing the integral area of the noise waveform by the integral area of the normal ECG waveform (Fig. 4(b)) with respect to the total time. In the calculation, the negative portion of the waveform was folded in the positive direction to calculate the ratio of the absolute integral values of the potential. The results in Fig. 4 show that the integral area of the noisy ECG was smaller than that of the normal ECG because the noise reduced the magnitude of the original ECG signal due to destructive interference. Therefore, motion-induced dynamic noise due to heart motion not only clearly reduces the magnitude of the original ECG signal, but also changes the shape of the P wave and QRS complex in the normal ECG waveform.

From the 3D skin-gel interface simulation model (Fig. 3), dynamic deformation of the skin and sol-gel layer was simulated numerically and the deformation rate was calculated based on the change in thickness of the two layers at points a

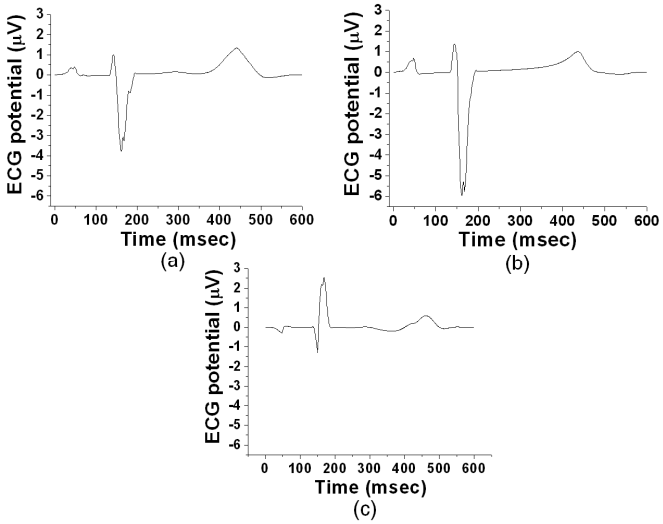

Fig. 4. (a) Dynamic noisy ECG potential for 3-cm vertical vibration motion at 5 Hz between points a and b (Fig. 1), (b) normal ECG waveform at rest, and (c) motion-induced dynamic noise waveform.

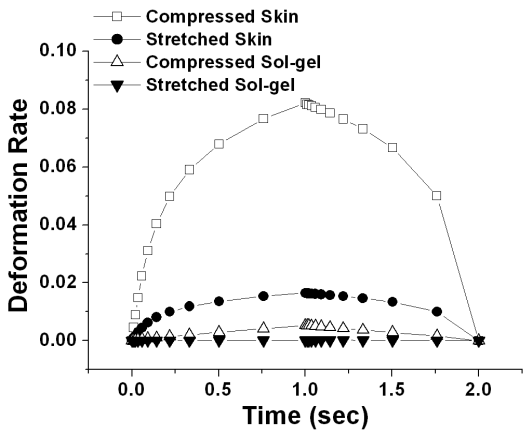

Fig. 5. Calculated dynamic deformation rates of the skin and sol-gel layers during ramp loading and unloading for 2 seconds for compressive and stretch motion, respectively.

and b (Fig. 3), as shown in Fig. 5. The results show that the deformation was nearly the same at the two points. The deformation of the skin layer was dominant for the compressive condition, while the stretch results did not produce a large change in thickness. The change in impedance according to the deformation rate of each layer was calculated for the compressive and stretch conditions and applied to the ECG simulation. The results showed that the ECG waveform under motion-induced deformation had a very small NSR, 0.0042 and 0.0006 for the compressive and stretch conditions, respectively, as shown in Table 2.

Table 2
NSR of the ECG waveforms due to skin-gel interface deformation

Deformation rate	*Skin*	0.015	0.1	0.5	0.9
	Sol-gel	14×10^{-5}	0.0055		
NSR		0.0006	0.0042	0.0214	0.0396

IV. DISCUSSION AND CONCLUSIONS

To determine the motion-induced noise level for different vibration motions of the heart, the NSR was calculated, as shown in Table 1 for different motion conditions of the heart. The interference of the motion-induced noise with the normal ECG was quite large, with an NSR > 0.41 for all cases, except for the 3-Hz cases. Moreover, the effects of motion were similar in both the horizontal and vertical directions. In particular, the 3-Hz motion showed relatively low interference. Therefore, the frequency of heart motion under dynamic conditions is a critical factor for the generation of motion-induced dynamic ECG noise.

In contrast, because the motion-induced noise due to skin-gel interface deformation was very minor, it was difficult to determine the critical range of the deformation rate that causes dynamic noise. The deformation rate was increased to 0.5 and 0.9 for the skin and sol-gel layers (Table 2) and the ECG was simulated with the corresponding impedance change at the skin-gel interface with the lumped parameter impedance model. This led to an increase in the dynamic noise level of 0.0214 and 0.0396 NSR (Table 2).

From these results, we concluded that the dynamic ECG noise with a wearable ECG measured within a local area is largely dependent on heart motion and motion frequency, while the effect of motion-induced deformation of the skin-gel interface is extremely small.

ACKNOWLEDGMENTS

This work was supported by Samsung Electronics. It was part of a study on the "Human Resource Development Center for Economic Region Leading Industry" Project, supported by the Ministry of Education, Science & Technology (MEST) and the National Research Foundation of Korea (NRF).

REFERENCES

[1] Y. D. Cha and G. Yoon, "Ubiquitous health monitoring system for multiple users using a ZigBee and WLAN dual-network", *Telemed J E Health,* vol. 15, pp. 891–897, Nov. 2009.

[2] W. Shin, Y. D. Cha, and G. Yoon, "ECG/PPG integer signal processing for a ubiquitous health monitoring system", *J Med Syst,* vol. 34, pp. 891–898, Oct. 2010.

[3] H. D. Kim, C. H. Min, and T. S. Kim, "Adaptable noise reduction of ECG signals for feature extraction", *Advances in Neural Networks, Lecture Notes in Computer Science,* vol. 3973, p. 586–591, 2006.

[4] Y. Lu, J. Yan, and Y. Yam, "A generalized ECG dynamic model with asymmetric gaussians and its application in model-based ECG denoising", *Biomedical Engineering and Informatics, 2009. BMEI '09. 2nd International Conference*, Oct. Tianjin, 2009, pp. 1–5.

[5] J. W. Lee and G. K. Lee, "Design of an adaptive filter with a dynamic structure for ECG signal processing", *International Journal of Control, Automation, and Systems*, vol. 3, no. 1, pp. 137–142, March 2005.

[6] S. Kawahito, H. Kitahata, K. Tanaka, J. Nozaki, and S. Oshita, "Dynamic QRS-complex and ST-segment monitoring by continuous vectorcardiography during carotid endarterectomy", *British Journal of Anaesthesia*, vol. 90, no. 2, pp. 142–147, 2003.

[7] R. Sameni, M.B Shamsollahi, C. Jutten, "Filtering electrocardiogram signals using the extended Kalman filter", *Proceedings of the 2005 IEEE Engineering in Medicine and Biology 27th Annual Conference*, Shanghai, China, September 1–4, 2005.

[8] R. Sameni, G. D. Clifford, C. Jutten, and M. B. Shamsollahi, "Multichannel ECG and noise modeling: application to maternal and fetal ECG signals", *EURASIP Journal on Applied Signal Processing*, vol. 2007, no. 1, pp. 94–108, Jan. 2007.

[9] A. Nygren, C. Fiset, L. Firek, J. W. Clark, D. S. Lindblad, R. B. Clark, and W. R. Giles, "Mathematical model of an adult human atrial cell: the role of K+ currents in repolarization", *Circ Res,* vol. 82, pp. 63–81, Jan 9–23. 1998.

[10] A. Bueno-Orovio, E. M. Cherry, and F. H. Fenton, "Minimal model for human ventricular action potentials in tissue", *J Theor Biol,* vol. 253, pp. 544–560, Aug., 2008.

[11] M. Potse, B. Dube, and A. Vinet, "Cardiac anisotropy in boundary-element models for the electrocardiogram", *Med Biol Eng Comput,* vol. 47, pp. 719–729, Jul., 2009.

[12] C. Flynn, A. Taberner, and P. Nielsen, "Mechanical characterisation of *in vivo* human skin using a 3D force-sensitive micro-robot and finite element analysis", *Biomech Model Mechanobiol*, vol. 10, pp. 27–38, April, 2011.